Study on true stress correction from tensile tests

Choung, J. M.[1],[*] and Cho, S. R.[2]

[1]*Hyundai Heavy Industries Co., LTD, Korea*
[2]*School of Naval Architecture and Ocean Engineering, University of Ulsan, Korea*

Abstract

Average true flow stress-logarithmic true strain curves can be usually obtained from a tensile test. After the onset of necking, the average true flow stress-logarithmic true strain data from a tensile specimen with round cross section should be modified by using the correction formula proposed by Bridgman. But there have been no firmly established correction formulae applicable to a specimen with rectangular cross section. In this paper, a new easy-to-use formula is presented based on parametric finite element simulations. The new formula requires only incremental plastic strain and hardening exponents of the material, which are simply presented from a tensile test. The newly proposed formula is verified with experimental data for high strength steel DH32 used in the shipbuilding and offshore industry and is proved to be effective during the diffuse necking regime.

Keywords: True flow stress; Logarithmic true strain; True stress correction; Bridgman equation; Diffuse necking; Flat specimen; Aspect ratio; Plastic hardening exponent

---

1. Introduction

Tensile tests of materials are used to obtain various elastic and plastic material properties such as elastic modulus, initial yield strength, ultimate strength, plastic hardening exponent, strength coefficient, etc. A true stress-logarithmic true strain curve for the material of concern, focused mainly on plastic properties, is necessarily required in order for numerical analyses accompanying large strain and fracture problems such as ship collision, ship grounding or fire explosion of FPSO.

Unfortunately, most engineers are interested in getting only a load-elongation curve from the tensile tests. Even with load-elongation data, however, it is impossible to estimate average true stress-logarithmic true strain data beyond the onset of the diffuse necking. Namely, an average true stress-logarithmic true strain curve estimated from a load-elongation curve is valid only until uniform deformation, viz., before the onset of necking. For most engineering steels, a non-uniform deformation field, called plastic instability, starts to develop just after a maximum load. At the same time, flow localization, called diffuse necking, starts at the minimum cross section of the specimen. The stress state and deformation in the necked region are analogous to those in the notch of a circumferentially notched round tensile specimen. For most steels, the load continuously decreases during diffuse necking, which terminates in ductile fracture of the specimen.

After a non-uniform deformation field develops in the necked region of a tensile specimen, an analytic solution [1] is widely used for true stress correction from the tensile specimen with a round cross section, hereafter denoted as round specimen. However, the Bridgman equation requires continuous data, which are diameter reduction and radius change in necked geometry. As a result, that can be the principal drawback to applying the Bridgman equation.

It is also known that the Bridgman equation is not

applicable for correction of average true stress-logarithmic true strain curve of tensile specimens with rectangular cross section, which is hereafter denoted as flat specimen, because the Bridgman equation is derived based on the assumptions of uniform strain distribution and axisymmetric stress distribution in the minimum cross section. Flat specimens are used as favorably as round specimens, due to convenience of machining or thin thickness of original material, even though there is no firmly established solution for stress correction like the Bridgman equation.

Aronofsky [2] pioneeringly investigated stress distribution at the necked region of two flat specimens and pointed out the stress pattern was not uniform in the minimum cross section of flat specimen. Unlike a round specimen, the initial aspect ratio (breadth/thickness) of a flat specimen involves the following two problems: determination of average true stress since area reduction is dependent on aspect ratio, and correction of average true stress since the stress state in the necked region is not uniform and dependent on aspect ratio. Zhang et al. [3] proposed a new formula about area reduction where thickness reduction of flat specimen should be measured. To derive the area reduction formula, numerical analyses were conducted for the flat specimens with various aspect ratios and hardening exponents. Based on the reference aspect ratio of 4 and reference thickness reduction of 0.5, the area reduction equation can be used to correct average true stress. A weighted average method for determining equivalent uniaxial true stress from average uniaxial true stress after onset of necking was presented for flat-shaped specimens by Ling [4]. This method requires a weight constant, which is not explicitly known for subject materials. Scheider et al. [5] also suggested a new formula that is related to the coefficient for average tensile stress correction. Like the equation of Zhang et al. [3], Scheider et al. [5] also carried out a series of numerical analyses, but the suggested formula is effective only for the thin flat specimens.

As a result, there is no firmly and explicitly established method or formula to correct true stress after necking of a flat specimen. This study presents a new formula to estimate true stress correction for flat specimens beyond onset of necking. At first, fundamentals and concepts related to the present study will be introduced in Section 2. Numerical analysis results will be shown in the first part of Section 3. Later in Section 3, a new formula will be derived based on

numerical study. Finally, the validity of the proposed formula will be reviewed and compared with experimental results in Section 4.

2. Fundamentals

2.1 Stress and strain before onset of necking

Fig. 1 schematically shows the typical engineering stress-engineering strain curve from a tension test with round specimen where three blocks are obviously seen. In Block 1, elastic and uniform deformation are undergoing up to the yielding point. During Block 2, deformation is still uniform, but the material experiences plastic deformation, which starts from the first yield point and ends at the onset of diffuse necking. The terminology 'Necking' usually means diffuse necking. Finally, in Block 3, non-uniform plastic deformation starts from the onset of diffuse necking and ends to fracture. The terminology 'Plastic Instability' comes from non-uniform plastic deformation phenomenon. For thinner flat specimens, a local shear band is usually formed on the necked surface of the plate specimen. This band is called "localized necking" and the onset of localized necking can be considered as fracture of the material since localized necking is usually short and rapidly terminates in a fracture.

Strain, describes quantitatively the degree of deformation of a material, measured most commonly with extensometers or strain gauges. During uniaxial deformation, engineering strain or nominal strain (e) can be generally expressed as Eq. (1).

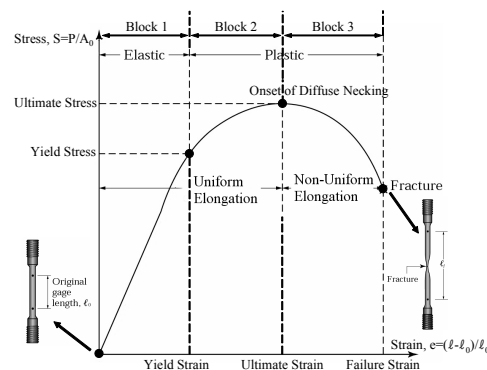$$e = \frac{\Delta L}{L_0} = \frac{L - L_0}{L_0} \tag{1}$$

Fig. 1. Engineering stress-strain representing three typical blocks in ductile metal specimen under tensile load.

Because of the nature of the irreversible process of plastic deformation, the deformation path is important together with the final configuration of the specimen. Therefore, an incremental approach is needed in plastic problems. Let dL be the incremental change in gauge length at the beginning of the corresponding increment; then, the corresponding tensile plastic strain increment ($d\varepsilon_p$) becomes

$$d\varepsilon_p = \frac{dL}{L} \tag{2}$$

The tensile plastic strain to the extent of elongation L is given by

$$\varepsilon_p = \int_{L_0}^{L} d\varepsilon_p = \int_{L_0}^{L} \frac{dL}{L} = \ln\frac{L}{L_0} \tag{3}$$

The strain defined by Eq. (3) is called the uniform true strain or natural strain. The uniform true strain is related to the engineering strain until onset of necking by Eq. (4) where A_0 and A, respectively, mean initial minimum cross sectional area and instantaneous minimum cross sectional area.

$$\varepsilon_p = \ln\frac{L}{L_0} = \ln\frac{A}{A_0} = 2\ln\frac{D}{D_0}$$
$$= \ln\frac{(L-L_0)+L_0}{L_0} = \ln(e+1) \tag{4}$$

Since stress describes quantitatively the degree of load acting on a material, engineering stress can be generally expressed as

$$S = \frac{P}{A_0} \tag{5}$$

Engineering stress is defined with reference to the initial configuration. If the reduction of the cross sectional area is large compared with the original sectional area, the engineering stress definition becomes inaccurate. For instance, it fails to predict strain hardening correctly. For more realistic stress definition, the instantaneous cross sectional area should be used. Before onset of necking, true stress is given by Eq. (6).

$$\sigma = \frac{P}{A} \tag{6}$$

$$A = A_0 e^{\varepsilon_p} \tag{7}$$

Eq. (7) comes from the assumption that the volume is conserved for the uniform true stress-engineering stress relationship. In other words, if no volumetric change beyond plastic deformation is assumed, then

$$AL = A_0 L_0 \tag{8}$$

Since $\ln L / \ln L_0 = \varepsilon_p$, then $A_0 / A = L / L_0 = e^{\varepsilon_p}$. Like Eq. (4), one may relate uniform true stress and engineering stress by

$$\sigma = S(1+e) \tag{9}$$

It is important to note that above equation holds only for uniform deformation, i.e., where stresses in every point across the minimum cross-section are the same. For the non-uniform case, average true stress is defined as Eq. (10).

$$\sigma = \lim_{\Delta A \to 0} \frac{\Delta P}{\Delta A} \tag{10}$$

It is very difficult to measure ΔP and ΔA independently, so this equation is considered solely as a definition and as a theoretical value. This implies that the uniform true flow stress can be directly obtained only when the deformation is uniform by measuring the force and the corresponding cross sectional area. Once deformation ceases to be uniform, only the average true flow stress can be measured and the stress distribution cannot be easily determined experimentally. This is the main reason for the problems encountered in the attempts to obtain equivalent true stress after onset of necking.

2.2 Considere's criterion

Diffuse necking is similar to axisymmetric necking under tension in a round specimen. Diffuse necking occurs in the manner of very gradual shape change and thickness/breadth reduction in flat specimens. Once localized necking is started, however, the breadth of the specimen changes little, but the thickness in the necking band shrinks rapidly.

The true stress-true strain curve, which should monotonically increase, can be approximated by the following power expression due to Hollomon:

$$\sigma = K(\varepsilon_p)^n \tag{11}$$

where K is the strength coefficient and n the work hardening exponent given by

$$n = \frac{d\ln\sigma}{d\ln\varepsilon_p} \tag{12}$$

From Hollomon's equation, Eq. (6) can be expressed as Eq. (13)

$$P = \sigma A = (K(\varepsilon_p)^n)(A_0 e^{\varepsilon_p}) \tag{13}$$

Considering the natural logarithm in both sides of Eq. (13),

$$\ln P = \ln K + n \ln \varepsilon_p + \ln A_0 + \varepsilon_p \tag{14}$$

Differentiating both sides of Eq. (14) with $d\varepsilon_p$, then

$$\frac{d \ln P}{d\varepsilon_p} = 0 + \frac{n}{\varepsilon_p} + 0 + 1 \tag{15}$$

The onset of necking takes place when the internal force reaches a maximum value, namely $d \ln P / d\varepsilon_p$ =0 in Eq. (15), and finally one can find that n is equal to ε_p which is called Considere's criterion.

$$\varepsilon_p \Big|_{onset\ of\ necking} = \varepsilon_p \Big|_{max.tensile\ load} = \varepsilon_u \tag{16}$$

According to Considere's criterion, diffuse necking starts at the point of maximum stress on the engineering stress-strain curve and the corresponding plastic strain is equal to the work hardening exponent n. Hence, the greater the strain-hardening exponent, the greater is the plastic strain to reach the diffuse necking. The physical meaning of hardening exponent n is the true strain at the onset of necking.

2.3 Stress and strain after onset of necking

During uniform deformation of a specimen, the stress state is uniaxial for both flat specimens and round specimens. However, after onset of necking, it is changed from uniaxial stress state to triaxial stress
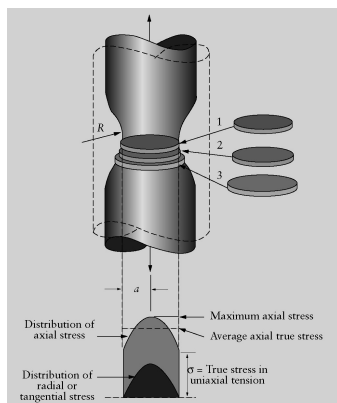

Fig. 2. Triaxial stress state in the necked region. R is radius of curvature in the necking line and a radius in the minimum cross section [6].

state as shown in Fig. 2.

In developing a method for finding the true stress-true strain relation beyond necking for a round specimen, Bridgman assumed uniform strain distribution in the necked section. In fact, strain distribution in the minimum cross section after necking is known to be not uniform. The radial plastic strain $\varepsilon_{p,r}$ in the minimum cross section is the same as the tangential plastic strain $\varepsilon_{p,t}$ and double the axial plastic strain $\varepsilon_{p,a}$.

$$\varepsilon_{p,r} = \varepsilon_{p,t} = \varepsilon_{p,a} / 2 \tag{17}$$

Based on this assumption, the equivalent plastic strain $\varepsilon_{p,eq}$ at the minimum cross section is equal to the axial strain $\varepsilon_{p,a}$ at the minimum cross section. Recalling equation (3), which corresponds to the volume conservation condition, $\varepsilon_{p,eq}$ becomes

$$\varepsilon_{p,eq} = \varepsilon_{p,a} = \ln\left(\frac{A_0}{A}\right) \tag{18}$$

Therefore, Eq. (18) is called average true strain, logarithmic true strain or Bridgman strain. From Eq. (18), it is relatively easy to get the logarithmic true strain at the necked minimum cross section by measuring the instantaneous reduction of the minimum cross section.

On the other hand, when a neck forms in a round specimen, the region at the minimum cross section tends to reduce more than the region just above and below the minimum cross section. As a result, the region above and below the minimum cross section constrains free reduction of region at the minimum cross section, and a triaxial stress state of hydrostatic stress develops at the region of minimum cross section. This hydrostatic stress does not affect plastic straining because no shear stress is involved in the necked region but contributes to increase the average true stress (P/A) for plastic flow, which is called average true stress (Eq. (19)). Increase of $\sigma_{a,av}$ due to hydrostatic stress gives a tip that the hydrostatic stress promotes fracture of the material.

$$\sigma_{a,av} = \frac{P}{A} \tag{19}$$

Due to the triaxial stress state in the necked cross section, average true stress $\sigma_{a,av}$ is not equal to the equivalent true stress σ_{eq}. Assuming proportional loading, Bridgman [1] derived the stress distribution in three components at the smallest cross section as

$$\sigma_r = \sigma_t = \frac{\sigma_{a,av}}{\left(1+\dfrac{2R}{a}\right)}\left\{\frac{\ln\left(\dfrac{a^2+2aR-r^2}{2aR}\right)}{\ln\left(1+\dfrac{a}{2}R\right)}\right\} \qquad (20)$$

$$\sigma_a = \frac{\sigma_{a,av}}{\left(1+\dfrac{2R}{a}\right)}\left\{\frac{1+\ln\left(\dfrac{a^2+2aR-r^2}{2aR}\right)}{\ln\left(1+\dfrac{a}{2}R\right)}\right\} \qquad (21)$$

Replacing Eqs. (20) and (21) into the von Mises yield function and vanishing shear stress term in the von Mises yield function, then equivalent true stress is presented by

$$\sigma_{eq} = \frac{\sigma_{a,av}}{\left(1+\dfrac{2R}{a}\right)\ln\left(1+\dfrac{a}{2R}\right)} = \sigma_{a,av}\cdot\zeta \qquad (22)$$

Eq. (22) physically means that the equivalent true stress at the minimum cross section can be derived with experimental data of tensile force P, area A, neck radius R and radius a. Actually, the correction parameter ζ should always be smaller than 1.0 after onset of necking. Although verification of this correction method is difficult because three components of stresses after onset of necking are not easily and directly measured, Bridgman's stress correction has been considered to give reliable approximation from many researches. For example, finite element analyses by Zhang and Li [7] showed that stress distribution in the minimum cross section approximately follows Bridgman's equation. Therefore, it is generally accepted that if a and R are accurately measured, Bridgman's correction method can predict the true stress-strain relation beyond necking fairly well in a specimen with round cross section. However, it must be noted that that Bridgman's correction is not easy to use in practice, as it requires the radius of curvature R and the minimum radius a, which are both difficult to measure with sufficient degree of accuracy, with increasing variation of tensile loading even for a round specimen. In order to overcome this difficulty, LeRoy et al. [8] proposed the ratio of a and R in the necked region where ε_u implies true strain when the internal force reaches a maximum value. Eq. (23) is known to be relatively accurate.

$$\frac{a}{R} = 1.1(\varepsilon_p - \varepsilon_u) \qquad (23)$$

3. Derivation of a new formula

As shown in Eq. (22), one of the principal objectives of this study is to determine the correction parameter ζ for flat specimens.

3.1 Finite element modeling

As shown in Fig. 3, the scantlings of the specimens representing FE models are as specified in many industrial standards such as ASTM [9], JIS [10] and KS [11]. All the specimens are modeled in one-eighth considering symmetry condition (Fig. 4). With a fixed breadth b_0 of 12.5 mm, aspect ratios are changed from one to five and additionally ten for observation of the effect of very high aspect ratio. As a result, six types of FE model with different aspect ratios are prepared. No intentional geometric imperfections to trigger diffuse necking are applied to all the FE models because the mesh density at the center of specimen is finer than that of the remaining part. No severe stress concentration like a hot spot is expected in tensile test simulation even after onset of necking, so the stress distribution is not much affected by mesh density in necked geometry. Translational constraints are, respectively, imposed on the nodes in the three symmetry plane. As an actuating force, prescribed displacements are applied to the nodes at the end of the grip. Eight node solid elements with reduced integration scheme are applied by using the Abaqus/Standard. In the authors' experiences, there would be little difference of results between full integration element (C3D8) and reduced integration element (C3D8R) in simulating a tensile test.

Since Hollomon's power law does not explain the behaviors close to initial yield stress, Ludwik's (Eq. (24)) or Swift's (Eq. (25)) power laws are recommended to be taken into account. In this study, Swift's power law is applied to FE model with σ_0 =235 MPa, E=200 GPa and ν =0.3 where iso-
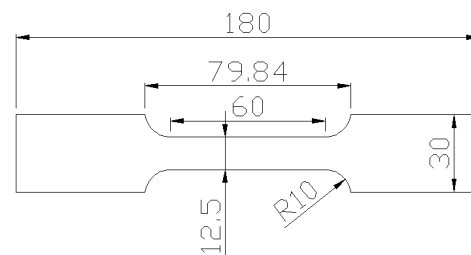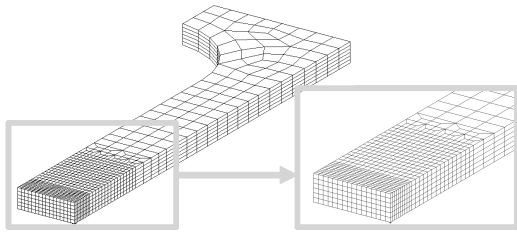

Fig. 3. Scantling of the flat specimen [mm].
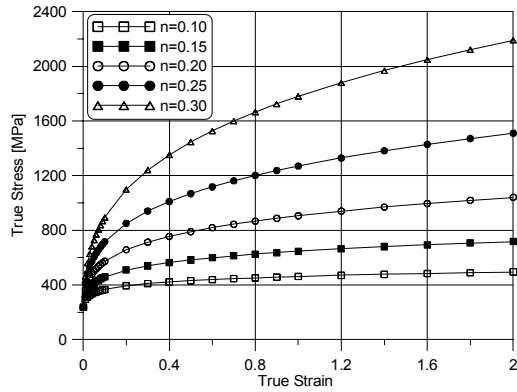
Fig. 4. Typical FE model of the flat specimen.

Fig. 5. True flow stress - logarithmic true strain curve for material input.

Fig. 6. Thickness-breadth reduction curves.

Fig. 7. Cushioning effect. b and t are reduced thickness and breadth.

tropic homogeneous materials are considered. To reduce modeling parameter, K is substituted by $\sigma_0/(\varepsilon_0)^n$ into Eq. (25).

$$\sigma = \sigma_0 + K(\varepsilon_p)^n \tag{24}$$

$$\sigma = K\left(\varepsilon_0 + \varepsilon_p\right)^n = \sigma_0\left(1 + \frac{\varepsilon_p}{\varepsilon_0}\right)^n \tag{25}$$

Plastic hardening exponents from 0.1 to 0.3 in increments of 0.05 are applied to Eq. (25). Totally, 30 FE models are prepared and analyzed in this study. Fig. 5 represents equivalent true flow stress-logarithmic true strain curves, which are used for material input of the FE model, according to various plastic hardening exponents. The considered plastic hardening exponents will cover most of the engineering steels used in shipbuilding and offshore construction, except special purpose austenitic materials like 304 stainless of which n is up to 0.45.

3.2 Finite element analysis results

3.2.1 Observation of reductions in thickness and breadth
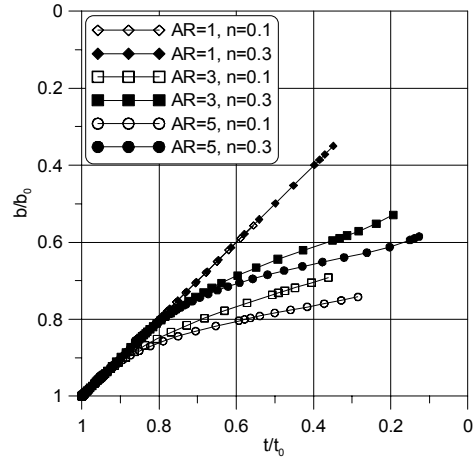
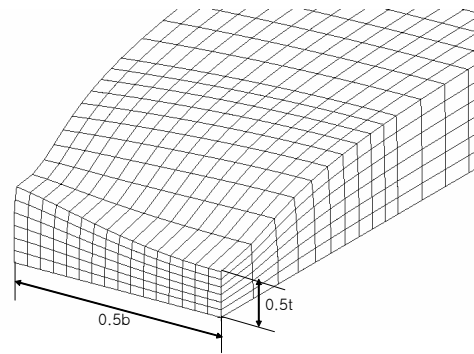Fig. 6 shows thickness-breadth reduction curves.

When the aspect ratio is 1.0, thickness and breadth reduction rates are the same regardless of hardening exponents. However, the bigger the aspect ratio or the smaller the plastic hardening exponent, the larger the thickness reduction than the breadth reduction. Therefore, for specimens with large aspect ratios and small plastic hardening exponents, early fracture is subject to occur.

Zhang et al. [3] perceived differences between two area reduction rates and considered thickness reduction rates to be a proportional reduction, of which concept is analogous to diametric reduction of a round specimen. In the authors' opinion, recovered thickness at the center of breadth direction does not completely represent thickness reduction because of cushioning effect as shown in Fig. 7. Scheider et al. assumed that even after onset of necking, $t/t_0 = b/b_0$ is effective. But this assumption is proved to be invalid during non-uniform deformation from Fig. 6, ex-

(a) Aspect ratio = 1.0, n = 0.1

(b) Aspect ratio = 1.0, n = 0.3

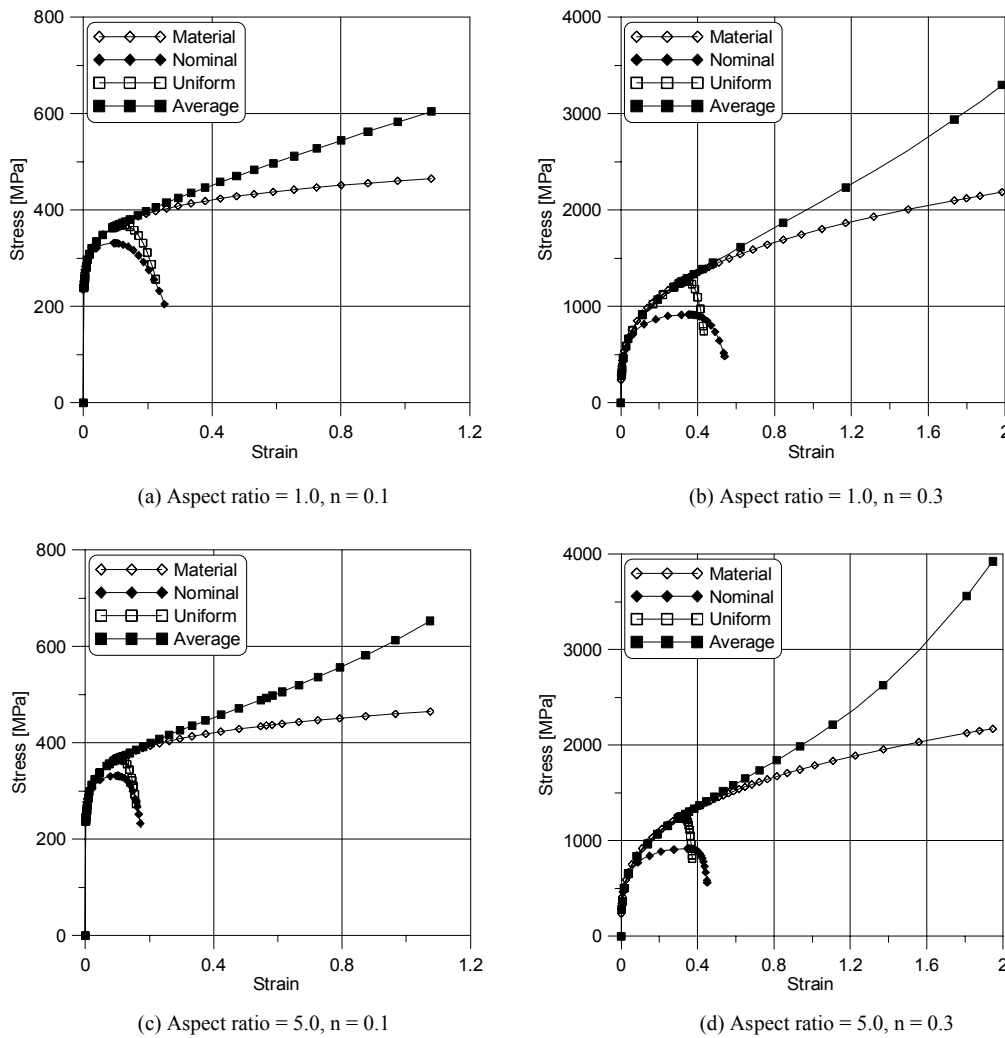(c) Aspect ratio = 5.0, n = 0.1

(d) Aspect ratio = 5.0, n = 0.3

Fig. 8. Comparison of stress - strain curves : material, nominal (engineering), uniform true and average true.

cept when initial thickness and breadth are identical.

3.2.2 Comparison between a nominal stress, uniform true stress and average true stress

Fig. 8 compares a specific material's equivalent true stress-logarithmic true strain curves with nominal stress-nominal strain, uniform true stress-uniform true strain and average true stress-logarithmic true strain curves. Material input means the stress-strain input data used for FE analysis. Nominal strain is calculated with nodal displacement from a surface node located at the center in breadth direction, which is 25mm apart from center in length direction (gage length= 50mm). Uniform true strain is calculated by Eq. (4) and uniform true stress by Eq. (9). In order to calcu-

late true logarithmic strain given by Eq. (19), a reduced area should be calculated for each increment of loading. The Gauss-Green equation is used to calculate a polygon of reduced perimeter bounded by dozens of nodes. Average true stress is calculated by using Eq. (19).

As expected, a nominal curve severely deviates from a material curve as soon as nominal stress is beyond yield stress. A uniform true stress-true strain curve coincides well with a material curve until the tensile force reaches a maximum value (ultimate stress), but after the maximum force, the uniform stress falls rapidly down showing much difference with the material curve. An average true stress-logarithmic true strain curve shows a similar trace

with the material one up to relatively large strain, but deviation between the average true curve and material curve increases, as plastic strain exceeds the hardening exponent. The main objective of this study is to attempt to fill the deviations between the average true curve and material curve.

3.2.3 Considere's criterion: validity of analysis

Since plastic strain at the maximum load ε_u is

Table 1. Comparison of flow stress ratios.

		Aspect Ratio					
		1.00	2.00	3.00	4.00	5.00	10.00
Hardening Exponent	0.10	1.00	1.00	1.00	1.00	1.00	1.00
	0.15	0.97	0.96	1.01	0.95	0.95	0.99
	0.20	1.00	1.00	1.00	1.00	1.00	1.00
	0.25	0.99	0.98	0.99	0.98	0.99	0.98
	0.30	0.98	1.00	1.00	1.00	1.00	1.00

equal to hardening exponent according to Considere's criterion, a comparison of the average true stress when the maximum force is reached and the average true stress when plastic strain equal to hardening exponent can be a good index to check the accuracy of the current analysis procedure. Table 1 shows a comparison for all analysis results where the numerator is the average true stress when maximum force is reached. Since the worst deviation between the maximum flow stress and flow stress when $\varepsilon_u = n$ is at most 5% for all cases, the present analysis procedures are thought to be reliable.

3.3 Derivation of a new correction parameter (ζ)

Fig. 9 represents plastic strain-correction parameter relationship for varying hardening exponents where plastic strain before onset of necking is not provided. It can be seen from Fig. 9 that for the same aspect ratio, even though the hardening exponents are different from each other, the correction parameters collapse into one curve until a specific plastic strain after which shear stresses at the symmetry plane increase

(a) n=0.1   (b) n=0.15   (c) n=0.2

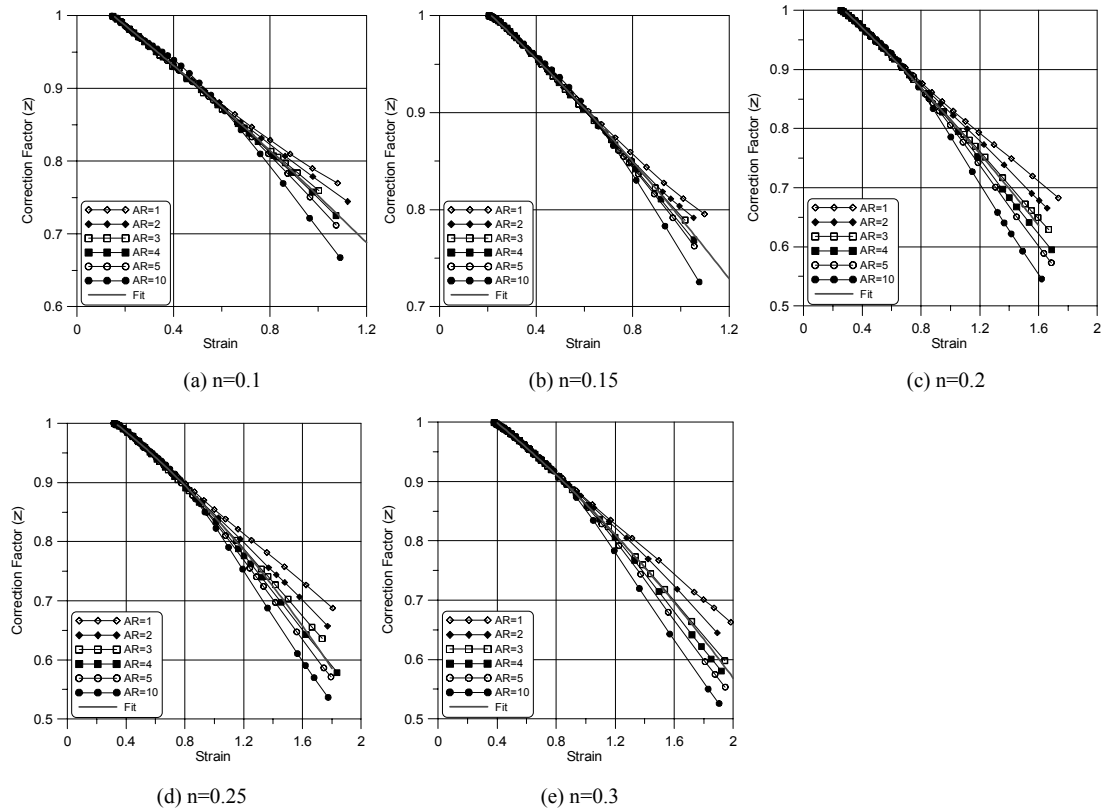(d) n=0.25   (e) n=0.3

Fig. 9. Plastic strain-correction parameter curves.

significantly and shear slant fracture starts to develop. Since it is impossible to simulate fracture with the current FEA scheme, the validity of the to-be proposed formula is confined before the onset of localized necking.

Instead of attempting to use a global multiple regression scheme, one can fit curves through two steps. As a first step, a second order polynomial, Eq. (26), is adopted to describe the plastic strain and correction parameter relationship from Fig. 9.

The value of 1.4 is the average of the first plastic strain values in Fig. 9 when the correction parameter is to be smaller than 1.0. Three coefficients of α, β and γ in the second order polynomial are individually obtained according to hardening exponents. It is noted that the above polynomial does not contain any dependency with hardening exponents. As a second step, based on coefficients obtained, dependencies are investigated between aspect ratio and polynomial coefficients. A linear regression model, Eq. (27), is used to represent the dependencies.

$$\zeta(\varepsilon_p) = \begin{cases} 1 & \text{for } \varepsilon_p \leq 1.4n \\ \alpha\varepsilon_p{}^2 + \beta\varepsilon_p + \gamma & \text{for } \varepsilon_p > 1.4n \end{cases} \quad (26)$$

$$\begin{aligned} \alpha &= -0.0704n - 0.027\tilde{5} \\ \beta &= 0.4550n - 0.2926 \\ \gamma &= 0.1592n + 1.024 \end{aligned} \quad (27)$$

Recalling Eq. (22), the equivalent true flow stress σ_{eq} is calculated by Eq. (28) where average uniaxial flow stress $\sigma_{a,av}$ is determined by tensile test, and correction parameter $\zeta(\varepsilon^p)$ is determined by Eq. (26) and Eq. (27).

$$\sigma_{eq} = \sigma_{a,av}\zeta(\varepsilon_p) \quad (28)$$

The formula proposed in this study is very easy to use for two reasons. First, the format of the formula is explicitly expressed as Eqs. (26), (27) and (28). Second, the proposed formula can be available with knowledge of the hardening exponent and incremental plastic strain values, which are determined by tensile test of a specimen.

4. Verification of the proposed formula

4.1 Test setup

Flat specimens are machined from thermo mechanically rolled steel plate BV-DH32 with 36mm

Table 2. Chemical composition of BV-DH32 steel.

C	Si	Mn	P	S	Cu	Ni	Cr	Mo
0.14	0.28	1.06	0.012	0.003	0.03	0.02	0.03	0.01

Table 3. Typical mechanical properties of BV-DH32 steel.

Minimum yield strength	Minimum tensile strength	Minimum elongation
315 (355) MPa	440 (480) MPa	22 (31) %

Table 4. Breadth and thickness in reduced section.

No.	b_0	t_0	b_0/t_0
P33	12.044	12.523	0.962
P34	12.030	9.000	1.337
P35	11.950	4.974	2.402

thickness. This grade of steel is almost exclusively utilized in shipbuilding for the construction of structural parts of ships and offshore platforms. From mill sheets for the mother plate, the chemical compositions are shown in Table 2. Typical mechanical properties at room temperature are summarized in Table 3 where the values in parentheses are from mill sheets for the mother plate.

As for parallel direction to rolling, three pairs of smooth flat specimens (P33, P34 and P35) are prepared so as to have different aspect ratios by changing thicknesses. Actual dimensions at the reduced section are listed in Table 4; the other dimensions are identical to Fig. 3. The experiments are conducted with a 300kN UTM with controlled displacement. With a gage length of 50mm, a constant loading speed of 1mm/min is applied. The loading is stopped every 1mm or 2mm extension of gage length to measure the actual thickness and breadth changes at the minimum cross section.

Thickness and breadth are manually measured, with digital calipers and micrometer, at the six longitudinally different points to search the minimum cross section even before the onset of necking. After the onset of necking, six points at the smallest cross section are measured for every increment due to the cushioning effect of specimens with rectangular cross section.

Square grids are stenciled on the surface of the breadth side of the specimen to analyze digital images recorded during every test increment (See Fig. 10). Digital images are taken with a digital camera with a resolution of 2816×2112 pixels. The camera is
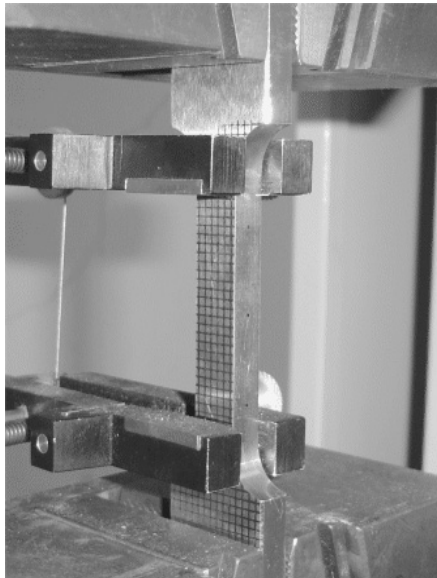
Fig. 10. A photo of test set up for specimen P34.

mounted on a digital height gage to keep consistent barrelling distortion due to lens convexity during elongation of the specimen.

4.2 Test results

Average uniaxial true flow stress-logarithmic true strain relations based on manual measurements are shown in Fig. 11(a), where it is noted that the curves for all specimens are almost coincident regardless of the aspect ratio of the flat specimen. Both breadth reductions determined from manual measurement and

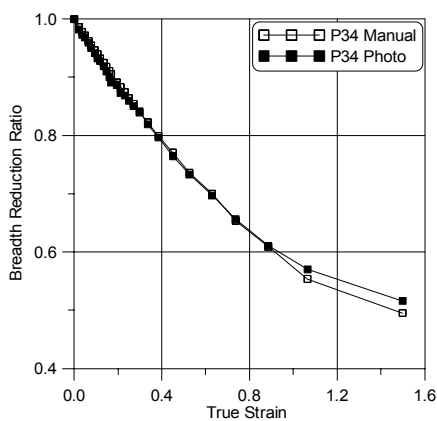Table 5. Measured mechanical properties of BV Grade DH32 steel.

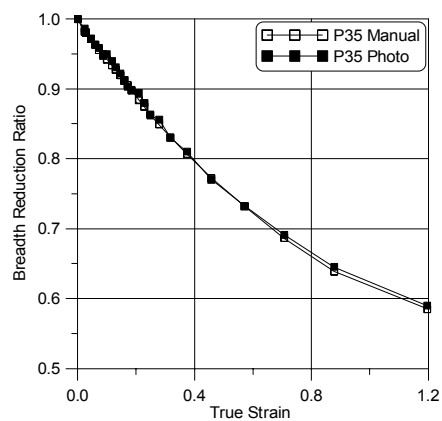|	σ_y [MPa]	σ_u [MPa]	n	K [MPa]	ε_f
P33	360.2	493.7	0.283	968.7	1.55
P34	358.0	494.0	0.263	938.9	1.50
P35	364.9	512.1	0.273	981.6	1.72
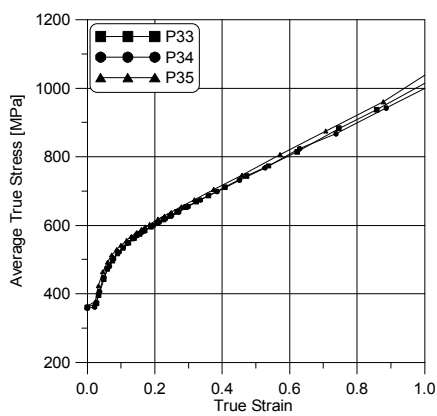
(a) Average true stress - strain curves
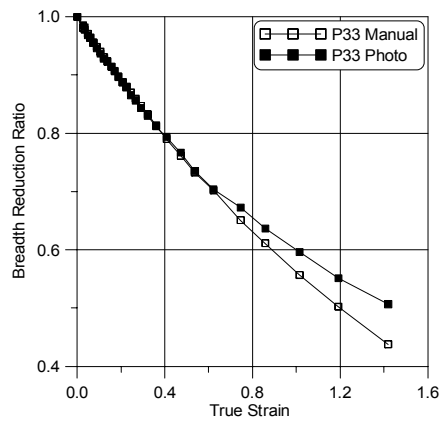
(b) Breadth reduction for P33

(c) Breadth reduction for P34

(d) Breadth reduction for P35

Fig. 11. Measured average true stress - strain curves and comparison of breadth reductions for test specimens.

(a) ε^p =0.41

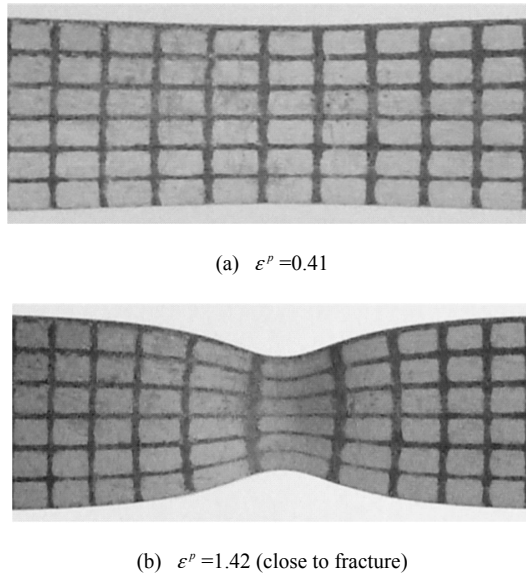(b) ε^p =1.42 (close to fracture)

Fig. 12. Moving grids in local necking zone.

digital image analyses are compared in Fig. 11(b), (c) and (d). Because the cushioning effect is most obvious for P33, which is close to unit aspect ratio, the deviation between manual measurement and photo analysis is increased for the specimens with the larger aspect ratio. The moving grids at ε_p =0.41 and ε_p =1.42 (just previous step of fracture) for P33 are represented in Fig. 12. The mechanical properties obtained from experiments are shown in Table 5 where the hardening exponent n and strength coefficient K are derived by using Hollomon's power law. On the other hand, true fracture strain is determined from measurements of actual area reductions.

4.3 Verification of proposed formula

Verification procedure is subdivided in the following steps:

(a) Preparation of average uniaxial true stress-logarithmic true strain data obtained from experiments

(b) Correction of the data in step (a) using the formula proposed (Eqs. (26), (27) and (28))

(c) FE analysis using corrected equivalent uniaxial true stress - logarithmic true strain

(d) Extraction of average uniaxial true stress - logarithmic true strain data from FE analysis

(e) Correction of the data in step (d) using the formula proposed

(f) Comparison of the data in step (a) and step (d)
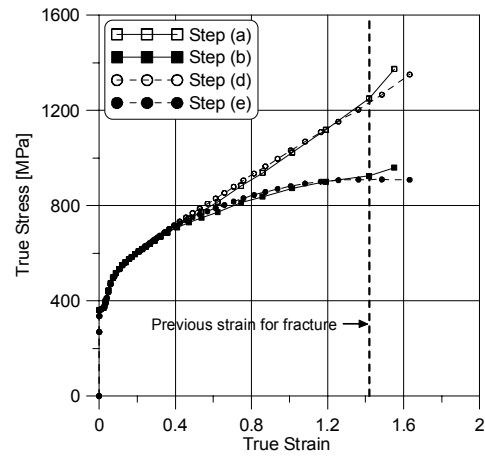
(a) P33
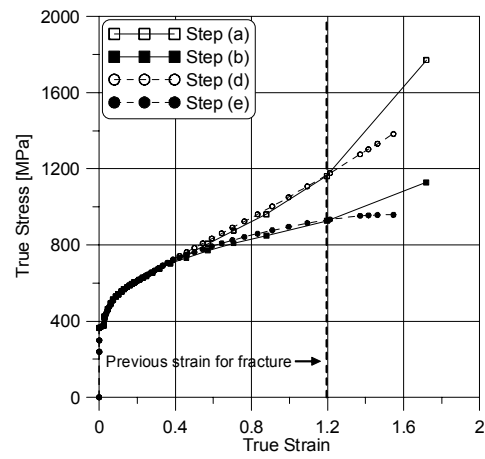
(b) P35

Fig. 13. Comparison of measured and calculated true stresses.

(g) Comparison of the data in step (b) and step (e)

After correction of the measured average true stress shown in Fig. 11(a), the corrected curve is used for material data of finite element analysis. As expected, the data in step (a) excellently coincide with the data in step (d) (Fig. 13). This covers specimens with largest and smallest aspect ratios. Both corrected curves in step (b) and step (e) are also in good agreement up to a very large strain of 1.2.

Scheider et al. (2004) have proposed a formula that contains two basic assumptions. One is the plane stress condition, which means Scheider's formula can only be applied to very thin specimens with large aspect ratio. The other assumption is that the breadth reduction ratio is equal to the thickness reduction ratio even after onset of necking. However, it is clear that

the stress state in the necked geometry is triaxial, not biaxial, even if a relatively thin specimen as shown in Fig. 13 and breadth reduction ratios tend to be larger than the thickness reduction ratio for a thin specimen (See Fig. 6).

5. Conclusions

In order to elucidate the necessity for stress correction parameter $\zeta(\varepsilon^p)$ after onset of necking, fundamental definitions related to Bridgman correction are introduced in Section 2 where the various definitions are described in detail.

Through extensive numerical analyses, a new formula for predicting equivalent uniaxial true stress is proposed to correct the average true stress obtained from tensile tests of flat specimens. The new formula requires following test data : average true flow stress and logarithmic true strain. To obtain the average true stress from a tensile test, the area reduction should be measured during the tensile test. It is somewhat difficult to measure area reduction from an experiment for flat specimens, so the formula by Zhang et al. [3] can be helpful for estimating average true flow stress-logarithmic true strain curve with only recorded load and thickness reduction.

The conducted numerical analyses cover from one to ten of the aspect ratio and from 0.1 to 0.3 of the plastic hardening exponent. A second order polynomial is used in the first step to derive the relationship between plastic strain and correction parameter. In the second step, the dependency between plastic hardening exponents and polynomial coefficients in the first step is investigated by using linear order regression. Therefore, regardless of the aspect ratio of the rectangular specimen, one can easily use the proposed formula with plastic logarithmic strain, average true stress and plastic hardening exponent determined from tensile test.

The proposed formula is verified with experimental data obtained from three specimens with different aspect ratios and the same material. It is proved that the proposed formula is definitely effective for both specimens with the smallest and the largest aspect ratio (P33 and P35). It is confirmed that the current manual measurements of area reduction are successfully carried out from the comparison of digital image analysis. However, due to the natural drawback of digital image analysis, breadth reduction considering cushioning effects after onset of necking can be diffi-

cult to obtain exactly.

Nomenclature——————————————

a	:	Minimum radius in necked section of round specimen
A	:	Instantaneous area of specimen
A_0	:	Initial area of specimen
b	:	Instantaneous breadth of flat specimen
b_0	:	Initial area of flat specimen
D	:	Instantaneous diameter of round specimen
D_0	:	Initial diameter of round specimen
e	:	Nominal (Engineering) strain
E	:	Elastic modulus of material
K	:	Strength coefficient
L	:	Instantaneous gage length
L_0	:	Initial gage length
n	:	Plastic hardening exponent
P	:	Uniaxial load
R	:	Radius of curvature in necked zone of round specimen
S	:	Nominal (Engineering) stress
t	:	Instantaneous thickness of flat specimen
t_0	:	Initial thickness of flat specimen
α	:	Quadratic order coefficient in second order polynomial
β	:	Linear order coefficient in second order polynomial
γ	:	Constant coefficient in second order polynomial
ε_f	:	True fracture strain
ε_p	:	Plastic strain
$\varepsilon_{p,a}$	:	Axial plastic strain in the minimum cross section
$\varepsilon_{p,r}$	:	Radial plastic strain in the minimum cross section
$\varepsilon_{p,t}$	:	Tangential plastic strain in the minimum cross section
$\varepsilon_{p,eq}$	:	Equivalent plastic strain in the minimum cross section
ε_u	:	True strain at maximum internal load
ε_0	:	Initial yield strain
v	:	Poisson ratio
σ	:	True flow stress
σ_a	:	Axial stress in the minimum cross section
σ_r	:	Radial stress in the minimum cross section
σ_t	:	Tangential stress in the minimum cross section
$\sigma_{a,av}$	:	Average axial true stress in the minimum cross section

σ_{eq} : Equivalent true stress in the minimum cross section

σ_u : True stress at maximum internal load

σ_0 : Initial yield stress

ζ : Stress correction factor

References

[1] P. W. Bridgman, Studies in Large Plastic Flow and Fracture, McGraw-Hill, New York, (1952).

[2] J. Aronofsky, Evaluation of stress distribution in the symmetrical neck of flat tensile bars, *J. Appl. Mech.* (1951) 75-84.

[3] K. S. Zhang, M. Hauge, J. Odegard and C. Thaulow, Determining material true stress-strain curve from tensile specimens with rectangular cross section, *Int. J. Solids Struct.* 36 (1999) 3497-3516.

[4] Y. Ling, Uniaxial true stress-strain after necking, *AMP J. Technology* 5 (1996) 37-48.

[5] I. Scheider, W. Brocks and A. Cornec, Procedure for the determination of true stress-strain curves from tensile tests with rectangular cross-section specimens, *J. Eng. Mater. Tech.* 126 (2004) 70-76.

[6] S. Kalpakjian and S. R. Schmid, Manufacturing Processes for Engineering Materials, Addison Wesley Publishing Co., (2001).

[7] K. S. Zhang and Z. H. Li, Numerical analysis of the stress-strain curve and fracture initiation for ductile material, *Engng. Fracture Mech.* 49 (1994) 235-241.

[8] G. LeRoy, J. Embury, G. Edwards and M. F. Ashby, A model of ductile fracture based on the nucleation and growth of voids, *Acta Metallurgica* 29 (1981) 1509-1522.

[9] ASTM E8, Standard Test Methods for Tension Testing of Metallic Materials, (2004).

[10] JIS Z 2201, Test Pieces for Tensile Test for Metallic Materials, (1998).

[11] KS B 0801, Test Pieces for Tensile Test for Metallic Materials, (1981).